

## Optimizing Heterogeneous Catalysts

**The Effect of Outer-Sphere Acidity on Chemical Reactivity in a Synthetic Heterogeneous Base Catalyst\*\***

*John D. Bass, Sandra L. Anderson, and  
Alexander Katz\**

Elegant examples of outer-sphere design to control chemical reactivity can be found in the active sites of biological catalysts.<sup>[1–5]</sup> Unlike biological systems, in which uniformity and isolation of the active site permit control and optimization of the outer sphere,<sup>[6]</sup> achieving the same in synthetic heterogeneous systems consisting of tethered organic functional groups has remained elusive. This is because such synthetic catalysts typically consist of a distribution of active sites that can range from subnanometer clusters to monolayers with macroscopic dimensions.<sup>[7–9]</sup> This distribution leads to nonuniform outer-sphere environments that are not amenable to rigorous control by synthetic manipulation.

---

[\*] Prof. A. Katz, J. D. Bass, S. L. Anderson  
Department of Chemical Engineering  
University of California at Berkeley  
Berkeley, CA 94720-1462 (USA)  
Fax: (+1) 510-642-4778  
E-mail: katz@cchem.berkeley.edu

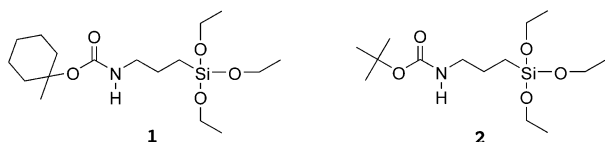
[\*\*] The authors thank Dow, Shell Foundation, and UC Berkeley Department of Chemical Engineering for financial support. J.D.B. is grateful to the Chevron Corporation for a graduate fellowship.



Supporting information for this article is available on the WWW under <http://www.angewandte.org> or from the author.

It would be highly desirable to use the framework surrounding an active site to define its outer sphere. Uniform active sites that are isolated from one another by the framework are expected to be most responsive to such an approach to outer-sphere control. Such active sites, each of which consists of a tethered organic functional group, can be synthesized by bulk silica imprinting.<sup>[10]</sup>

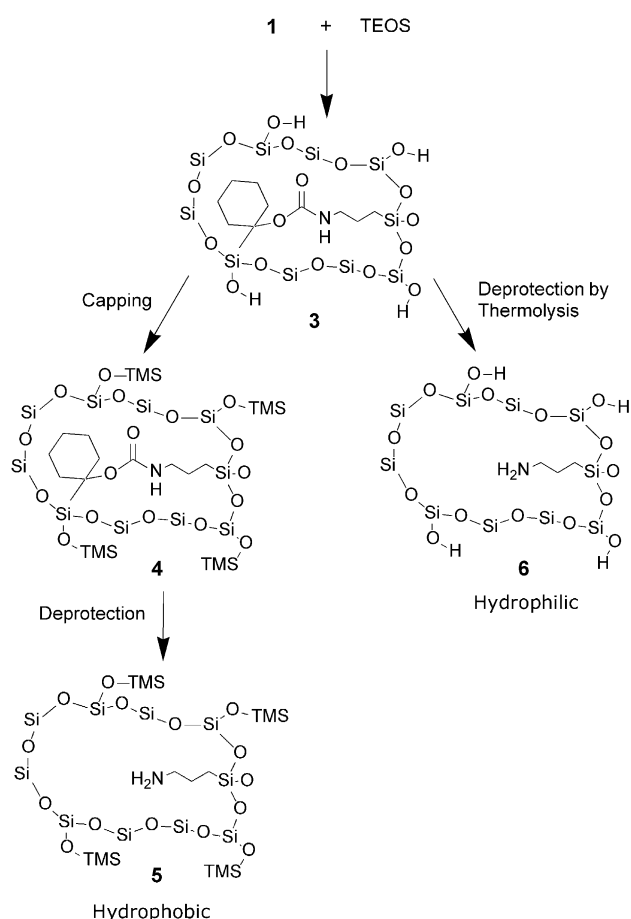
Recently, we developed a strategy for synthesizing bulk imprinted silica that permits the direct comparison of materials that are otherwise identical except for their framework composition at surface defect sites.<sup>[11]</sup> Here this strategy is used to systematically study the role of the framework as an outer sphere in a synthetic heterogeneous base catalyst. The results are demonstrated for three model chemical transformations, which are discussed in order of increasing mechanistic complexity: the position of equilibrium for intramolecular proton transfer between tautomers, the kinetics of an intramolecular chemical reaction without catalytic turnover, and the kinetics of an intermolecular catalytic reaction.



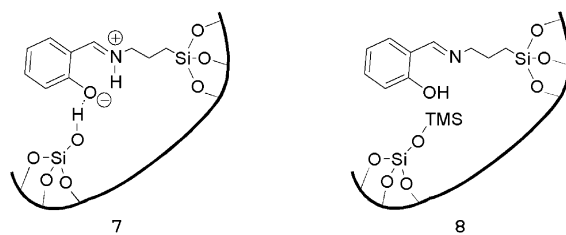
The imprinting approach is based on imprints **1** and **2** and is illustrated in Scheme 1. Imprint **1** was co-condensed with tetraethyl orthosilicate (TEOS) to form hybrid organic–inorganic sol–gel material **3**. Hydrophobic material **4** was prepared from **3** by capping framework silanol groups with trimethylsilyl groups. Subsequently, the imprint fragment was removed by carbamate deprotection to form **5**. The hydrophilic analogue **6** was prepared directly from **3** by thermolytic deprotection.<sup>[11]</sup> The same procedure was performed with imprint **2**.

The effect of the framework on intramolecular proton transfer equilibrium was investigated by treating imprinted amines in **5** and **6** with the chromophore salicylaldehyde, which affords reaction products that are amenable to UV/Vis characterization. Previous studies have observed strong solvent effects in analogous imines derived from salicylaldehyde, which give rise to product absorption bands at 400–450 nm corresponding to a zwitterionic product on dissolution in acidic protic solvents, and bands at 320–350 nm corresponding to a neutral phenolic product on dissolution in aprotic solvents.<sup>[12]</sup> These bands were used to characterize the polarity of alkali-exchanged zeolites by measuring the ratio of absorbance intensities at the corresponding wavelengths.<sup>[12–14]</sup> Our previous results show that the presence of acidic silanol hydrogen-bond donors stabilizes the zwitterionic form **7** ( $\lambda = 400\text{--}450\text{ nm}$ ) over the neutral phenolic form **8** ( $\lambda = 320\text{--}350\text{ nm}$ ).<sup>[11]</sup> Accessible acidic silanol groups are present in **6**, whereas they should be almost absent in **5**.

Figure 1 shows the diffuse reflectance UV/Vis spectra of **5** and **6** after treatment with salicylaldehyde. The marked effect of outer-sphere acidity is shown by the strong band at 400 nm for the imino group in **6** and by the substantial absence of this



**Scheme 1.** Hydrophilic and hydrophobic materials prepared by an imprinting approach. Both materials are derived from the same material **3**, which was synthesized from an acid–base-catalyzed sol–gel hydrolysis and condensation. Framework capping with hydrophobic TMS groups gave **4**, and subsequent deprotection yielded hydrophobic material **5**. Direct thermolysis of **3** yields hydrophilic material **6**.



band and the band at 320 nm for the imino group in **5**. This provides compelling evidence that neutral form **8** is present and is thermodynamically preferred in the hydrophobic environment of **5**. In contrast, the zwitterionic form **7** is thermodynamically favored in the hydrophilic environment of **6**.<sup>[11]</sup> This demonstrates thermodynamic control of a chemical reaction by varying the framework outer sphere.

In a separate experiment, we measured kinetic effects by determining the activation energy for thermolysis of immobilized imprint in **3** and **4**. Although mechanistically more complex than the proton transfer, the thermolysis of carbamates **3** and **4** is expected to be accelerated by the presence of

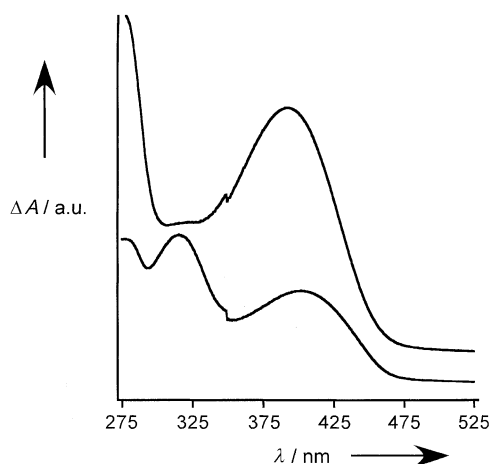


**Figure 1.** Solid-state diffuse-reflectance UV/Vis spectra of **5** (lower) and **6** (upper) containing a covalently bound solvchromatic indicator. The upper spectrum shows a pronounced zwitterion band on treatment with salicylaldehyde. The lower spectrum shows a strong band from the phenolic form of the indicator.

accessible silanol groups in the outer sphere because of the known acid lability of such carbamates. A related phenomenon has been demonstrated in homogeneous thermolysis of *N*-arylcabamates of tertiary alcohols, for which the activation energy for thermolysis decreases by approximately 6 kcal mol<sup>-1</sup> between decane and the protic solvent decanol.<sup>[15]</sup>

Thermogravimetric analysis (TGA) was used to measure the activation energy for thermolysis of the immobilized imprint. The difference in the temperature required for thermolysis on **3** and **4** is apparent from the data shown in Figure 2. Here, the hydrophobic material **4** reaches maximum thermolysis rates at 237°C, while this occurs at 170°C for hydrophilic material **3**. This temperature difference of 67°C reflects a significant change in the activation energy for

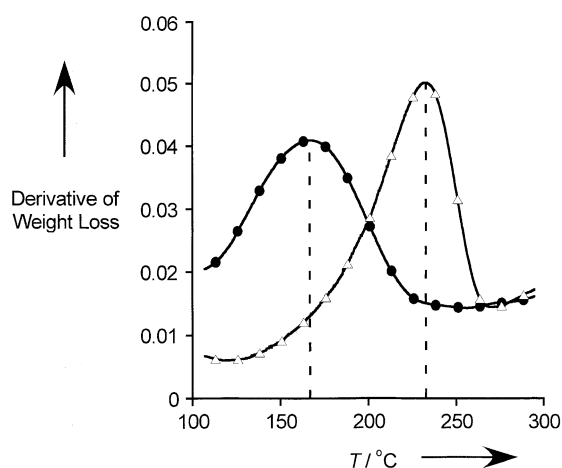


**Figure 2.** Rate of mass loss during thermolysis of carbamate, as measured by thermogravimetric analysis on hydrophobic **5** (Δ) and hydrophilic **6** (●). The dashed vertical lines are included for visual clarity, to indicate the temperature at which the maximum rate of thermolysis occurs. Data are shown for a constant heating rate of 1 °C min<sup>-1</sup>. The rate of mass loss is given in wt% °C<sup>-1</sup>.

thermolysis between **3** and **4**. The activation energy of thermolysis can be calculated directly from the data in Figure 2, according to the method of Redhead.<sup>[16]</sup> The activation energy thus calculated for **3** is 24.8 ± 0.3 kcal mol<sup>-1</sup>, while for **4** it is 29.0 ± 0.3 kcal mol<sup>-1</sup>. As expected for a system that is limited solely by chemical kinetics, as opposed to transport, these values were essentially unchanged by variations in heating rate, and particle and sample sizes. These results show that the acidic outer sphere in **3** reduces the activation barrier for thermolysis by about 4 kcal mol<sup>-1</sup> relative to that of **4**. These activation energies are consistent with previously reported activation energies for the olefin-forming step in the thermolysis mechanism, which is thought to be rate-limiting.<sup>[15]</sup> Similar effects have been observed with imprinted materials derived from **2**.

Finally, we measured the effect of the framework on an intermolecular chemical reaction involving catalytic turnover. We chose the Knoevenagel condensation of isophthalaldehyde and activated methylene compounds, because it was previously shown to be catalyzed by a primary amine on silica.<sup>[7,10,17,18]</sup> Our hypothesis was that the acidic outer sphere surrounding the primary amine in **6** should lead to higher catalytic rates than the hydrophobic outer sphere in **5**. This hypothesis is consistent with previously observed rate enhancements in Knoevenagel condensations when using heterogeneous catalysts in protic solvents,<sup>[19]</sup> as well as when using acid–base bifunctional catalysts.<sup>[8]</sup>

The conversion of isophthalaldehyde in reactions with malononitrile and ethyl cyanoacetate on base catalysts **5** and **6** is shown in Figure 3. Table 1 shows a summary of the turnover frequency (TOF) based on initial isophthalaldehyde conversion rates for reactions with malononitrile and ethyl cyanoacetate. The results for a commercially available catalyst, consisting of a monolayer of 3-aminopropyl groups on the surface of silica, are also shown. There is a large rate enhancement for **6** relative to both **5** and the commercially available surface-functionalized material. For the malononitrile system, the enhancement of **6** over **5** is a factor of about 50; for the ethyl cyanoacetate system, it is a factor of 25. Notably, the rate enhancement of **6** over the surface-functionalized catalyst is 30 for malononitrile and 90 for ethyl cyanoacetate. Background catalysis on the framework is insignificant, and these data are also shown for the use of **3** and **4** prior to carbamate deprotection as catalysts. The results demonstrate a significant outer-sphere effect on catalysis caused by modifications of the acidity of the silica framework surrounding each active site. We have observed similar rate accelerations with materials derived from imprint **2**.

Rational design of the outer sphere by framework modifications should accelerate improvements of heterogeneous catalysts. Our results illustrate this powerful approach for the specific case of an amine base catalyst tethered on silica. This approach is currently being extended to the control of chemical reactivity in other synthetic heterogeneous catalysts.

## Experimental Section

Salicylaldehyde binding: Imprinted silica (30 mg) was added to a solution of salicylaldehyde (2.65 mL, 0.005 M, 2 equiv) in acetonitrile

**Table 1:** TOFs for Knoevenagel condensation of isophthalaldehyde with malononitrile or ethyl cyanoacetate with **5**, **6**, and commercially available surface-functionalized catalysts. TOF is given in events per minute per catalytic site.

No.	Catalyst	Initial TOF [site <sup>-1</sup> min <sup>-1</sup> ]	
		Malononitrile	Ethyl cyanoacetate
Materials synthesized from imprint <b>1</b>			
1	hydrophobic <b>5</b>	0.10 ± 0.01	0.011 ± 0.002
2	hydrophilic <b>6</b>	4.7 ± 0.4	0.26 ± 0.04
Control materials			
7	Aldrich aminopropyl surface-functionalized silica	0.14 ± 0.01	0.0029 ± 0.0005
8	hydrophilic <b>3</b>	0.13 <sup>[a]</sup>	0.022 <sup>[a]</sup>
9	hydrophobic <b>4</b>	0.0023 <sup>[a]</sup>	0.0007 <sup>[a]</sup>

[a] TOF in hydrophilic and hydrophobic materials without amines (materials consisting of carbamates prior to deprotection) were calculated by assuming an amine number density corresponding to that in the deprotected materials.

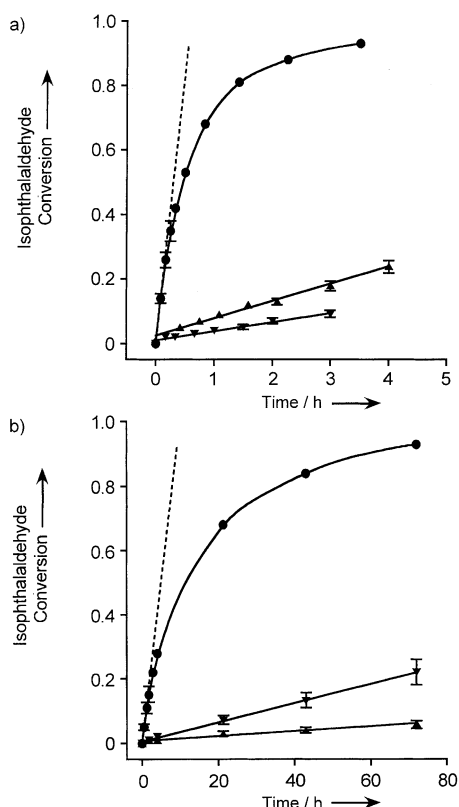


**Figure 3.** Fractional conversion of isophthalaldehyde as a function of time for base-catalyzed Knoevenagel condensation with a) malononitrile and b) ethyl cyanoacetate. Framework differences between hydrophilic catalyst **6** (●) and hydrophobic catalyst **5** (▼) lead to significant effects in the observed rate of reaction. Also shown (▲) is a commercially available surface-functionalized material consisting of a monolayer of aminopropyl groups grafted onto the surface of mesoporous silica. Dashed lines were used to calculate the initial rate in determining the TOF.

with stirring at room temperature. After the materials had equilibrated and formed the covalently bound imine chromophore on > 80 % of the amino groups, as monitored by gas chromatography, the materials were collected by filtration, washed with acetonitrile (100 mL), chloroform (100 mL), and pentane (50 mL), and subsequently Soxhlet-extracted in chloroform for 16 h.

Activation energy measurements: TGA was conducted with heating rates varying from 0.13 to 10 °C min<sup>-1</sup> on samples weighing between 2 and 15 mg. Materials (average particle size of 2 or 10 μm)

were placed on platinum pans and analyzed under a nitrogen flow of 20 mL min<sup>-1</sup>. Average particle diameter was estimated by scanning electron microscopy.

Knoevenagel condensation: A typical reaction was conducted with 10 mg of catalyst (the amount of catalyst was fixed at 0.005 molar equivalents of amine relative to isophthalaldehyde) in 20 mL an anhydrous benzene solution of concentration 0.022 M in isophthalaldehyde and 0.044 M of either malononitrile or ethyl cyanoacetate (reactor-vessel volume was 30 mL). The reaction with malononitrile was performed at room temperature (22 °C), while the reaction with ethyl cyanoacetate was performed at 40 °C. Aliquots were taken by syringe and analyzed by gas chromatography.

Received: June 23, 2003 [Z52181]

**Keywords:** heterogeneous catalysis · imprinting · sol-gel processes · supported catalysts

- [1] E. Breslow, F. R. N. Gurd, *J. Biol. Chem.* **1962**, 237, 371.
- [2] *Annual Review of Biochemistry*, Vol. 36 (Ed.: P. D. Boyer), Annual Reviews Inc, Palo Alto, **1967**.
- [3] T. K. Harris, G. J. Turner, *IUBMB Life* **2002**, 53, 85–98.
- [4] C. F. Barbas III, A. Heine, G. Zhong, T. Hoffmann, S. Gramatikova, R. Björnstedt, B. List, J. Anderson, E. A. Stura, I. A. Wilson, R. A. Lerner, *Science* **1997**, 278, 2085–2092.
- [5] A. Karlstrom, G. Zhong, C. Rader, N. A. Larsen, A. Heine, R. Fuller, B. List, F. Tanaka, I. A. Wilson, C. F. Barbas III, R. A. Lerner, *Proc. Natl. Acad. Sci. USA* **2000**, 97, 3878–3883.
- [6] M. Inoue, H. Yamada, T. Yasukochi, R. Kuroki, T. Miki, T. Horiuchi, T. Imoto, *Biochemistry* **1992**, 31, 5545–5553.
- [7] E. Angeletti, C. Canepa, G. Martinetti, P. Venturello, *Tetrahedron Lett.* **1988**, 29, 2261–2264.
- [8] A. Corma, S. Iborra, I. Rodríguez, F. Sánchez, *J. Catal.* **2002**, 211, 208–215.
- [9] M. E. Davis, A. Katz, W. R. Ahmad, *Chem. Mater.* **1996**, 8, 1820–1839.
- [10] A. Katz, M. E. Davis, *Nature* **2000**, 403, 286–289.
- [11] J. D. Bass, A. Katz, *Chem. Mater.* **2003**, 15, 2757–2763.
- [12] W. Turbeville, P. K. Dutta, *J. Phys. Chem.* **1990**, 94, 4060–4066.
- [13] P. K. Dutta, W. Turbeville, *J. Phys. Chem.* **1991**, 95, 4087–4092.
- [14] I. Casades, M. Alvaro, H. Garcia, M. N. Pillai, *Eur. J. Org. Chem.* **2002**, 2074–2079.
- [15] S. J. Ashcroft, M. P. Thorne, *Can. J. Chem.* **1972**, 50, 3478–3487.
- [16] P. A. Redhead, *Vacuum* **1962**, 12, 203–211. Similar results can be obtained by using another model by Kissinger: H. E. Kissinger, *Anal. Chem.* **1957**, 29, 1702–1706.
- [17] M. L. Kantam, P. Sreekanth, *Catal. Lett.* **1999**, 57, 227–231.
- [18] E. C. Angeletti, C. Canepa, G. Martinetti, P. Venturello, *J. Chem. Soc. Perkin Trans. 1* **1989**, 105–107.
- [19] P. Laszlo, *Acc. Chem. Res.* **1986**, 19, 121–127.